Pharmaceutical Research, Vol. 26, No. 8, August 2009 (© 2009)
DOI: 10.1007/s11095-009-9911-5

Research Paper

The *In vitro* Sub-cellular Localization and *In vivo* Efficacy of Novel Chitosan/GMO Nanostructures containing Paclitaxel

W.J. Trickler,[1] A.A. Nagvekar,[1] and A.K. Dash[1,2]

Received February 6, 2009; accepted May 11, 2009; published online May 20, 2009

Purpose. To determine the *in vitro* sub-cellular localization and *in vivo* efficacy of chitosan/GMO nanostructures containing paclitaxel (PTX) compared to a conventional PTX treatment (Taxol®).
Methods. The sub-cellular localization of coumarin-6 labeled chitosan/GMO nanostructures was determined by confocal microscopy in MDA-MB-231 cells. The antitumor efficacy was evaluated in two separate studies using FOX-Chase (CB17) SCID Female-Mice MDA-MB-231 xenograph model. Treatments consisted of intravenous Taxol® or chitosan/GMO nanostructures with or without PTX, local intra-tumor bolus of Taxol® or chitosan/GMO nanostructures with or without PTX. The tumor diameter and animal weight was monitored at various intervals. Histopathological changes were evaluated in end-point tumors.
Results. The tumor diameter increased at a constant rate for all the groups between days 7-14. After a single intratumoral bolus dose of chitosan/GMO containing PTX showed significant reduction in tumor diameter on day 15 when compared to control, placebo and intravenous PTX administration. The tumor diameter reached a maximal decrease (4-fold) by day 18, and the difference was reduced to approximately 2-fold by day 21. Qualitatively similar results were observed in a separate study containing PTX when administered intravenously.
Conclusion. Chitosan/GMO nanostructures containing PTX are safe and effective administered locally or intravenously. Partially supported by DOD Award BC045664

KEY WORDS: cancer; chitosan; gmo; nanostructure; paclitaxel.

INTRODUCTION

Paclitaxel (PTX) has been one of the best anti-neoplastic agents discovered in recent decades, and has been used for an extensive variety of malignancies, but its clinical application has been limited because of poor aqueous solubility (0.6 mM) and poor oral bioavailability (1). To date, only two commercial formulations have been developed. The oldest intravenously administered formulation developed uses 1:1 mixture of Cremophor EL to increase the solubility of paclitaxel (7 mM) (2). However, the solvent causes serious adverse side effects like severe hypersensitivity, neurotoxicity, nephrotoxicity and hypotensive vasodilation (3–5). These solvent related toxicities are in addition to, paclitaxel side effects like nausea, vomiting, hypersensitivity, bone marrow depression and arrhythmias (5,6). The newest formulation, Abraxane, is an injectable suspension of albumin-bound paclitaxel nanoparticles (7,8). However, bone marrow suppression is not only the dose dependant and dose limiting toxicity, but also neuropathy toxicity has been shown to be remarkably increased when compared to the traditional PTX formulation (9,10).

Current trends in paclitaxel research have concentrated on the development of alternative delivery systems to sustain the release of paclitaxel at or around malignant tissues in avoidance of the systemic toxic side-effects associated with paclitaxel and its formulations. One possible method to achieve this paradigm is to passively target tumor tissues through the over-expression of cell surface moieties. The over-expression and under glycosylation of mucin-1 antigen is one of the early hallmarks of tumorigenesis. Almost all human epithelial and non-epithelial cell adenocarcinomas, multiple myeloma, and some B-cell lymphomas exhibit an over-expression of mucin-1 (11). Chitosan has been shown to have bioadhesive and/or mucoadhesive properties due to interactions with the mucous membranes associated with epithelial barriers and tumors both *in vitro* (12–14) and *in vivo.* (15–19). We previously reported the use of a mucoadhesive nanoparticle formulation to increase the solubility of paclitaxel and subsequently increase the *in vitro* cellular accumulation and effectiveness of paclitaxel in MDA-MB-231 human breast cancer cells. The chitosan/GMO formulation reported in these studies incorporated paclitaxel in a chitosan/glyceryl monooleate (GMO) bioadhesive delivery system significantly increasing the cellular accumulation and efficacy of paclitaxel in MDA-MB-231 cells (20). Bioadhesive delivery systems are formulated to enhance drug bioavailability by increasing the

[1] Department of Pharmacy Sciences, School of Pharmacy and Health Professions, Creighton University Medical Center, 2500 California Plaza, Omaha, Nebraska 68178, USA.
[2] To whom correspondence should be addressed. (e-mail: adash@creighton.edu)

residence time and subsequent absorption through adhesion with the cellular surface. These studies clearly demonstrated surface-bound chitosan/GMO formulation, but the evidence and mechanisms of internalization and the *in vivo* efficacy remained to be elucidated.

This report investigates both the *in vitro* cellular mechanism responsible for the increased cellular accumulation of the chitosan/GMO formulation and the *in vivo* efficacy of the chitosan/GMO formulation previously reported. The current studies proposed the cellular mechanism for internalization was determined to be an endo-lysosomal internalization with nuclear co-localization of the chitosan/GMO formulation. In addition, the current report demonstrates a significant increase in the *in vivo* efficacy for the chitosan/GMO formulation following local or intravenous administration when compared to conventional available clinical formulation for paclitaxel.

MATERIALS AND METHODS

Materials and Reagents

All materials and reagents were obtained from commercial sources. Paclitaxel (PTX) was purchased from InB: HauserPharmaceutical Services Inc. (Denver, CO). The clinical paclitaxel formulation was purchased from Creighton University Medical Center pharmacy. FOX Chase SCID Female Mice with CB17 background (7 weeks old) mice were purchased from Charles Rivers Laboratories. MDA-MB-231 breast cancer cell line was purchased from American Type Culture Collection (ATCC) (Manassas, VA). The Gibco brand cell culture media and constituents, RPMI 1640, fetal bovine serum (FBS), penicillin/streptomycin, trypsin-EDTA and L-glutamine, were purchased from Invitrogen (Carlsbad, CA). Glyceryl monooleate (GMO) was obtained from Eastman Chemical Company (Kingsport, TN). Anhydrous citric acid was purchased from Acros Organics (Fairlawn, NJ). Acetonitrile (HPLC), methanol (HPLC), ammonium acetate (HPLC), sodium phosphate monobasic, sodium phosphate dibasic, hydrochloric acid (reagent grade), and Falcon tissue culture flasks were purchased from Fisher Scientific (Fairlawn, NJ). Low molecular weight chitosan was purchased from Aldrich Chemical Company (Milwaukee, WI). Veterinarian grade ketamine/xylazine was purchased from Sigma RBI (St. Louis, MO).

Preparation and Characterization of Paclitaxel Polymeric Nanostructures

The preparation and characterization of these polymeric nanoparticles (NPs) have been well documented and previously described by multiple emulsion and solvent evaporation methods (20). Briefly, a known amount of paclitaxel (4.5% w/total-w) or 6-coumarin (6-CM) (1% w/total-w) was incorporated into the fluid phase of GMO (1.75 ml at 40°C). The GMO mixture was emulsified with 12.5 ml of polyvinyl alcohol (0.5% w/v) (mw 30000–70000) by ultrasonication (18 watts for 2 min) (Sonicator 3000, Misonix, Farmingdale, NY). The initial emulsion was further emulsified with a chitosan solution (12.5 ml)(2.4% w/v) dissolved in citric acid (100 mM) by ultrasonication (18 watts for 2 min). The final emulsion is frozen (−80°C) prior to solvent evaporation by freeze drying methods (−52°C and < 0.056 mBar pressure) (FreeZone, Labconco, St Louis, MO). The mean particle size, size distribution and mean zeta potential of the nanoparticles were determined using a zetameter (ZetaPlus, Brookhaven Instruments Corporation, Holtsville, NY). Briefly, the nanoparticles were resuspended in deionized water (0.4 mg/ml) in triplicate and analyzed for particle size and zetapotential. The percent drug loading was calculated and expressed as a ratio of amount of drug extracted from the polymer matrix to the total weight of the nanoparticles. The HPLC analysis for PTX was achieved on a C18 Zorbax column (150 × 4.6 mm, 5 um) (Phenomenex, Torrance, CA) with a mobile phase consisting of acetonitrile, methanol, 0.1M ammonium acetate (48.5:16.5:35% v/v/v) at a flow rate of 0.75 ml/min. The effluents were monitored at 227 nm and quantified using the area under the peak from standard solutions dissolved in mobile phase (0.4 to 2 μg/ml).

Intracellular Association and Uptake of the Chitosan/GMO Formulation

The intracellular uptake of the chitosan/GMO formulation in MDA-MB-231 human breast cancer cells was evaluated by the HPLC method previously mentioned (21). In these studies, the cell monolayers were cultured in standard 6-well tissue culture plates at a seeding density of 500,000 cells per square centimeter and cultured until confluency in a humidified chamber at 37°C in RPMI-1640 growth media supplemented with 10% FBS, 1% L-glutamine and 1% penicillin/streptomycin. Confluent cell monolayers were treated with a single bolus suspension of chitosan/GMO formulation loaded with 6-coumarin (1 mg/ml) for various times (15–60 min). The cell monolayers were washed three times with ice cold PBS and lysed with 1% triton-X. The cell monolayer lysates were assayed for total protein content by the BCA method prior to freeze-drying. The freeze dried cell monolayer lysates were re-suspended in acetonitrile and centrifuged at 14,000 RPM in a microcentrifuge. The supernatant was analyzed by HPLC and the amount of Coumarin-6 was determined (Shimadzu SP-10A VP, Columbia, MD). The mobile phase was acetonitrile: Heptanesulfonic acid (70:30 (v/v)) and the flow rate was maintained at 0.2 mL/min. A Novapac C18 column (150 × 2.0 mm, Waters) with fluorescent detection at excitation 505 nm and emission 535 nm and quantified using the area under the peak from standard solutions dissolved in mobile phase (2–10 μg/ml). The cellular uptake data is presented as coumarin-6 amount per mg protein.

Chitosan/GMO Formulation Sub-Cellular Localization by Confocal Microscopy

The *in vitro* cellular association and sub-cellular localization of the delivery systems were evaluated in MDA-MB-231 human breast cancer cells. In these studies, cell monolayers were cultured on Falcon multi-well slides. Briefly, the cell monolayers were seeded in a multi-well cell culture slide at a density of 10,000 cells per well and incubated overnight in a humidified chamber at 37°C in RPMI-1640 growth media supplemented with 10% FBS, 1% L-glutamine and 1% penicillin/streptomycin. The cell monolayers were treated with the Chitosan/GMO formulation loaded with coumarin-6 as a function of time (15–30 min) in assay buffer

II spiked with 50 nM lysotracker red or Texas-Red transferrin. The cell monolayers were washed three times in ice cold PBS, fixed with glutaraldehyde (1%) and further stained with mounting media consisting of DAPI (1.5 ug/ml), n-propyl gallate (0.1 g) in PBS buffered glycerol. The wells were removed and coverslips placed and sealed. The slides were viewed at the Nebraska Center for Cell Biology confocal microscope facility at Creighton University.

Localized Chitosan/GMO Formulation Compared to a Conventional Formulation Following Systemic Administration

Briefly, FOX Chase SCID Female Mice with CB17 background (7 weeks old) mice were purchased from Charles Rivers Laboratories. MDA-MB-231 human breast cancer cells were cultured as previously described. On the day of injections, MDA-MB-231 cells were collected and re-suspended (30 million cells/ml) in RPMI 1640 serum free media. The mice received an injection (0.1 ml) in the fourth inguinal mammary pad and another subcutaneous injection (0.1 ml) in the ipsilateral flank. Both the mammary pad and the flank tumor development along with the animal weight were monitored at various intervals throughout the entire study. On day 14, the mice were randomly separated into four groups for treatment as follows: control (no treatment), PTX standard clinical IV solution (15 mg/kg) tail vein, (one dose each day for 3 days), placebo (blank formulation at 15 mg/kg, total formulation weight), PTX (4.5% w/w) chitosan/GMO formulation (15 mg/kg, total formulation weight). Therefore, the total PTX dose for the nanoparticle formulation was empirically determined to be 0.625 mg/kg by HPLC analysis. The rationale for selecting this dose was based on the previous *in vitro* studies demonstrating placebo effects for the nanoformulation at equivalent doses above 15 mg/kg total formulation weight (20). The theoretical dose was based on the calculation of a nanoparticle dose of 15 mg/kg with a drug load of 4.5% (w/w) (15 ×.045= 0.675 mg/kg). The nanoparticle formulations were suspended in sterile water just prior to injection. On day 14, each animal received the respective treatment by either intravenous or localized intratumoral injection in both tumors. On day 21, a second dose was administered. The data is expressed as mean tumor diameter ± SEM, n=6.

Intravenous or Localized Chitosan/GMO Formulation Compared to a Conventional Formulation Following Systemic or Localized Administration

The *in vivo* studies described in the previous section (section: Localized Chitosan/GMO Formulation compared to a Conventional Formulation following Systemic Administration) did not address the efficacy of the nanostructures when administered via an iv route, placebo effect of nanostructure when injected by an iv route, and efficacy of intratumoral injection of PTX solution. Therefore, this *in vivo* study was designed to address these above mentioned effects in the same *in vivo* xenograft model. Briefly, in these studies, FOX Chase SCID Female Mice with CB17 background (7 weeks old) mice were purchased from Charles Rivers Laboratories. MDA-MB-231 human breast cancer cells were cultured, and inocculated as previously described. Both the mammary pad and the flank tumor development along with the animal weight were monitored at various intervals throughout the entire study. On day 9, the mice were randomly separated in to six groups for treatment as follows: control (no treatment), PTX standard clinical IV solution (15 mg/kg) tail vein, one dose each day for 3 days in one group or 0.625 mg/kg administered locally in another group, placebo (blank chitosan/GMO formulation) (15 mg/kg, total formulation weight) tail vein, one dose each day for 3 days, PTX (4.5% w/w) chitosan/GMO formulation (15 mg/kg, total formulation weight) administered as either a single bolus dose locally in one group or 15 mg/kg, total formulation weight) tail vein in another group, one dose each day for 3 days. The group receiving a local dose of 0.625 mg/kg was derived from a calculation involving the maximum dose of nanoparticles used in the study, and the drug load in the nanoparticles. Since the maximum dose used was 15 mg/kg and the nanoparticles have a drug load of 4.5% (w/w) the calculated equivalent dose was 0.675 mg/kg (15×0.45=0.675 mg/kg). Therefore, the total PTX dose for the chitosan/GMO formulation was calculated to be 0.675 mg/kg. However, the dose was empirically determined to be 0.625 mg by HPLC analysis of 15 mg of nanostructure containing a theoretical PTX load of 4.5 % (w/w). The nanoparticle formulations were suspended in sterile water just prior to injection. On day 9, each animal received the respective treatment either intravenous or localized intratumoral injection in both tumors. The data is expressed as mean tumor diameter ± SEM, n=6.

End-point Tumor Histological Evaluation Intravenous or Localized Chitosan/GMO Formulation Compared to a Conventional Formulation Following Systemic or Localized Administration

At the end of the efficacy studies, the tumors were excised and placed in a micro-centrifuge tube and fixed with a formalin solution. Representative samples were sent to Creighton University Medical Center Clinical Pathology for machine processing. Briefly, the formalin fixed samples were dehydrated (80%, 90%, 95%×3, 100%×3, 1:1 ethanol:Xylene, Xylenex3) 15 min each, and embedded in paraffin, sectioned in 10mm sections using a Leitz model 1512 microtome and placed on standard microscope slides, and allowed to air dry overnight. The slides were deparaffinized in xylene (3×15 min) and rehydrated in ethanol (100%×3, 95%×1, 80%×1, deionized water) 5 min each. Hydrated sections were stained with hematoxalin for one minute, rinsed in DI water. Developed slides were de-stained (70% ethanol, 1% HCl, ten dips, and two 2 min wash tap water), and stained in alcoholic eosin-Y for 3 min, and rinsed and dehydrated in ethanol washes (95%×3, 100%×3 for 3 min each) and cleared in Safeclear tissue clearing agent (Fisher Sci. 314–629). Cleared slides were blotted and coverslips were mounted over tissue sections using Permount mounting media, and allowed to dry overnight.

Statistical Analyses

The results are expressed as means ± standard error of the mean (SEM) for all quantitative data. The analytical data was statistically analyzed where appropriate using single

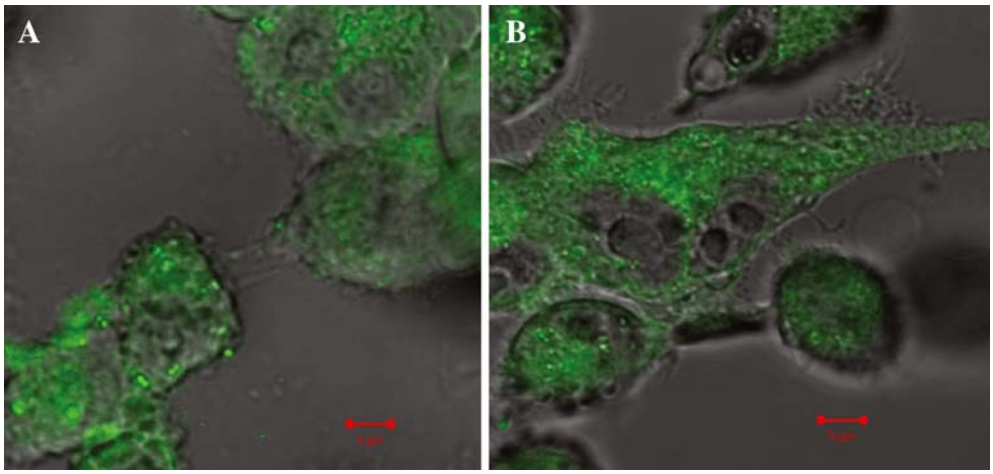

Fig. 1. The cellular association a chitosan/GMO formulation containing coumarin-6 in MDA-MB-231 cells. MDA-MB-231 Human Breast Cancer Cells Were Exposed to Courmarin-6 loaded Chitosan/GMO formulation for A) 15 min or B) 30 min.

factor analysis of variance followed by Tukey multiple post hoc test for paired comparisons of means (SPSS 10, SPSS Inc., Chicago, IL). For all studies, statistical significance was designated as $p<0.05$, unless otherwise stated.

RESULTS

Intracellular Association and Uptake of the Chitosan/GMO Formulation

The intracellular association and uptake of a coumarin-6 loaded chitosan/GMO formulation (1 mg/ml) were examined both quantitatively and qualitatively by confocal microscopy (Fig. 1) and HPLC (Fig. 2). Fig. 1 represents qualitative assessment using a confocal microscopy and Fig. 2 represents the quantitative data determined by using HPLC anlysis. The confocal micrographs show discrete time-dependent extracellular and intracellular vesicular images at both time points (15 and 30 min) (Fig. 1). As a control, the release of the fluorescent dye from the chitosan/GMO formulation in phosphate buffered saline was examined by standard USP methods and found to be negligible (< 0.1%) at both pH 4 and pH 7 over a 4 h experimental period (Data not shown). The quantitative HPLC studies clearly demonstrate the time dependent uptake of chitosan/GMO nanoparticles (Fig. 2).

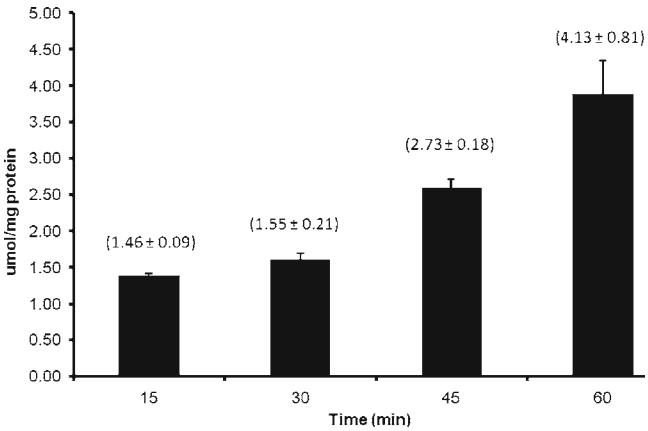

Fig. 2. Time dependent uptake of a chitosan/GMO formulation containing coumarin-6. Confluent MDA-MB-231 monolayers were exposed to a chitosan/GMO formulation containing coumarin-6 (1 mg/ml) for various time intervals (15 to 60 min). The results are presented as mean ± SEM (μmol/mg cellular protein) from three monolayers. The percentages of accumulated dose are provided above each bar as mean ± SD from three monolayers.

Chitosan/GMO Nanoparticle Sub-Cellular Localization by Confocal Microscopy

The sub-cellular localization of a coumarin-6 loaded chitosan/GMO formulation (1 mg/ml) was examined qualitatively by confocal microscopy (Fig. 3). The confocal micrographs show a rapid discrete time-dependent intracellular localization of chitosan/GMO nanostructures (Fig. 3). The combined images of the green nanostructures with the red lyso-tracker dye demonstrate a rapid co-localization of coumarin-6 loaded nanostructures within the intracellular lysosomal vesicles as early as 2 min. In addition, the rapid intracellular co-localization increased with time with green fluouescent structures appear within the cytoplasm suggesting either lysosomal saturation or escape at later time points (15 and 20 mins) (Fig. 3). Furthermore, in separate studies, nuclear co-localization was also observed by the combine images of a coumarin-six loaded chitosan/GMO formulation with the blue DAPI stained nuclear material in MDA-MB-231 cells (Fig. 4a and b). Observable free intracellular and co-localized green fluorescent coumarin-6 loaded nanostructures with the lysosomal vesicles and the nuclear material was determined (Fig. 4c).

Localized Chitosan/GMO Formulation Compared to a Conventional Formulation Following Systemic Administration

The efficacy of the chitosan/GMO formulation was compared to systemic administration of a conventional paclitaxel

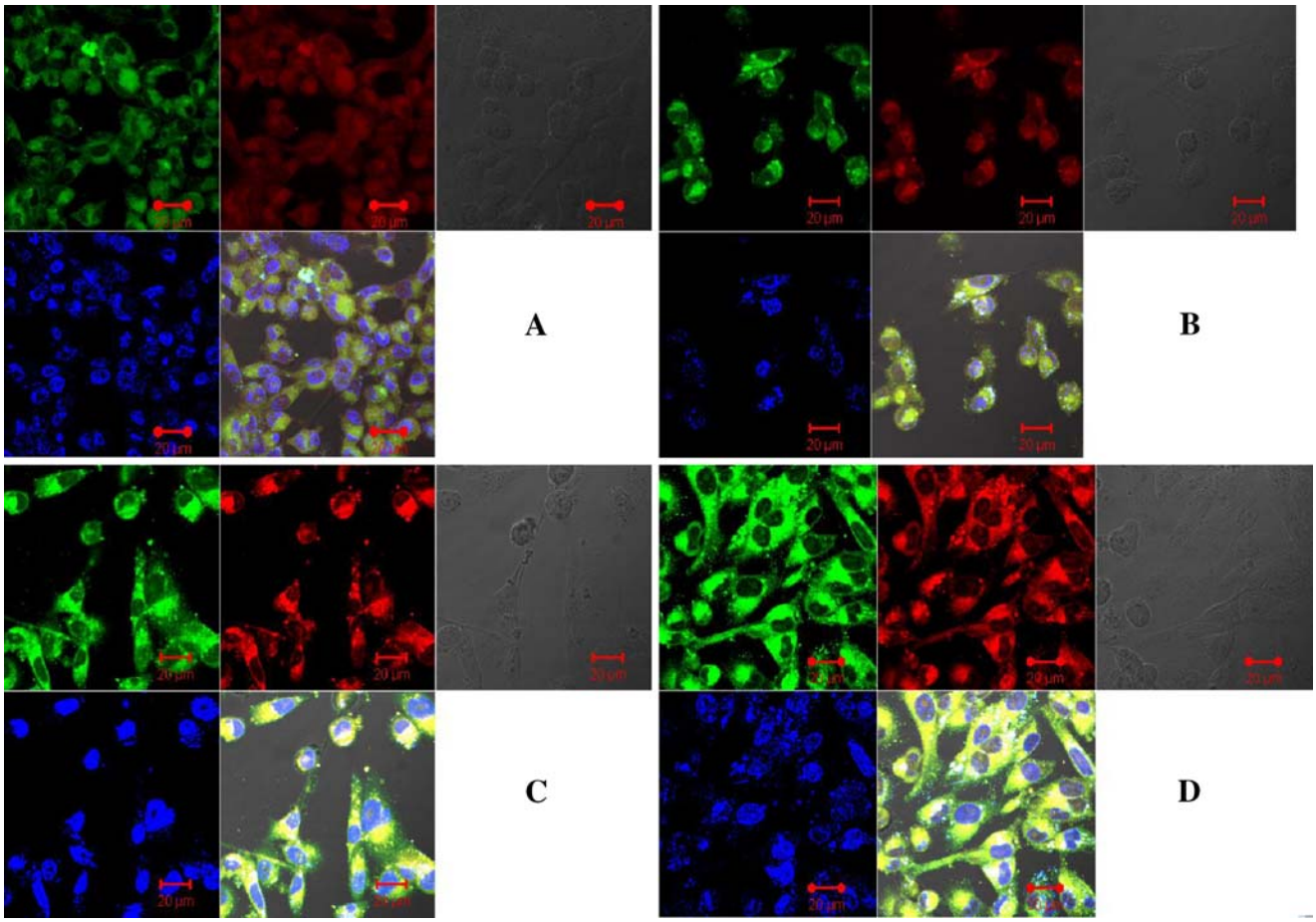

Fig. 3. Sub-cellular localization of a chitosan/GMO formulation containing coumarin-6. MDA-MB-231 human breast cancer cells were exposed a chitosan/GMO formulation containing coumarin-6 and the sub-cellular localization was examined by confocal microscopy for various time intervals (2, 5, 10 or 20 min). The green fluorescent dye coumarin-6 was combined with the red lyso-tracker dye, the blue fluorescent dye DAPI and contrast light following various exposure times A) 2 min, B) 5 min, C) 10 min and D) 20 min.

formulation in SCID mice following inoculation of MDA-MB-231 cells (Fig. 5a and b). After the initial MDA-MB-231 cell injection, tumor development was visible after 6 days and measurable on day 9 (Fig. 5a and b). The tumor diameter increased at a constant rate for all the groups between day 7 and day 14 (Fig. 5a and b). After a single intratumoral bolus dose of the PTX formulated nanoparticles, a significant decrease (50%) in tumor diameter in both the mammary pad and the flank was observed on day 15 when compared to control, placebo and PTX administered intravenously (Fig. 5a and b). At four days post treatment, the tumor diameter reached the maximal decrease in diameter to approximately 72% in both the mammary pad and the flank when compared to control, placebo and conventional PTX administered intravenously (Fig. 5a and b). Even though, the tumor shrinkage reached a significant reduction in diameter by day 18 in both the mammary pad and the flank, the difference was reduced to approximately 50% by day 21 in both the mammary pad and the flank when compared to control, placebo and PTX administered intravenously (Fig. 5a and b). At this point in the study, all the groups received a second treatment on day 21 (Fig. 5a and b).

Intravenous or Localized Chitosan/GMO Formulation Compared to a Conventional Formulation Following Systemic or Localized Administration

After the initial MDA-MB-231 cell injection, tumor development was visible after 7 days and measurable on day 9 (Fig. 6a and b). The tumor diameter increased at a constant rate for all the groups between day 7 and day 9 (Fig. 6a and b). After a single intratumoral bolus dose or intravenously administered PTX formulated nanoparticles, a significant decrease (65%) in tumor diameter in both the mammary pad and the flank was observed on day 14 when compared to control, placebo and PTX administered intravenous or a single intratumoral bolus (Fig. 6a and b). At fourteen days post treatment, the tumor diameter reached the maximal decrease in diameter to approximately 71% in both the mammary pad and the flank when compared to control, placebo and PTX administered intravenous or a single intratumoral bolus (Fig. 6a and b). Even though, the tumor shrinkage reached and maintained a significant reduction in diameter until day 24 in both the mammary pad and the flank, the difference was reduced to approximately 50% by day 28 in both the mammary pad and the flank when

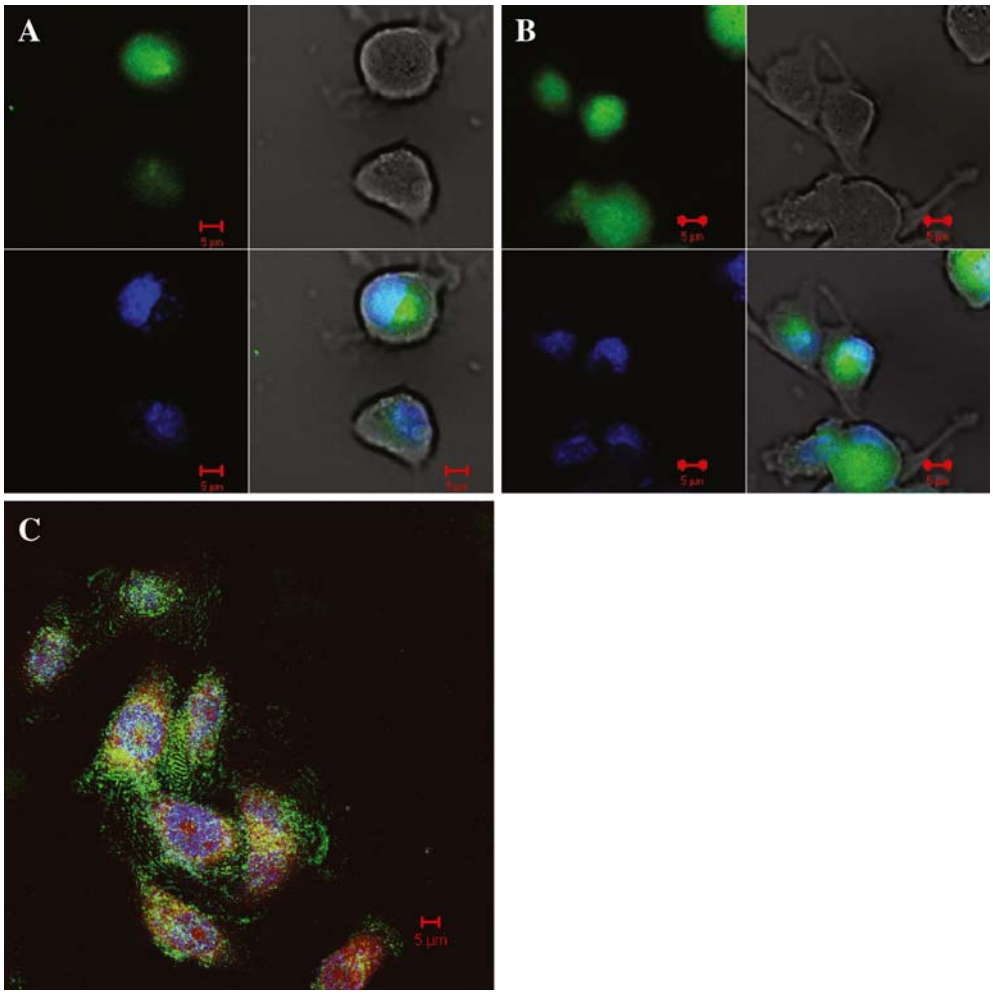

Fig. 4. A chitosan/GMO formulation nuclear Co-localization MDA-MB-231 human breast cancer cells were exposed a chitosan/GMO formulation containing coumarin-6 and the nuclear co-localization was examined by confocal microscopy. **a**) or **b**) The green fluorescent dye coumarin-6 was combined with the blue fluorescent dye DAPI and light microscopy following 30 min exposure. **c**) The green fluorescent dye coumarin-6 was combined with a red fluorescent lyso-tracker dye and the blue fluorescent dye DAPI following a 30 min exposure.

compared to control, placebo and PTX administered intravenous or a single intratumoral bolus (Fig. 6a and b). The mean rate of tumor growth was significantly reduced following the either intra-tumor or intravenous administration of chitosan/GMO nanostructures containing paclitaxel (Table I).

End-point Tumor Histological Evaluation

At the end of the efficacy studies, the tumors were excised and histologically evaluated by H & E staining methodology (Figs. 7 and 8). In support of the efficacy studies, the histological studies also show a remarkable decrease in either flank tumors (Fig. 7) or mammary tumors (Fig. 8) following the either local or intravenous administration of the paclitaxel chitosan/GMO formulation compared to the conventional paclitaxel formulation. In the case of intravenous administered chitosan/GMO formulation containing paclitaxel, there was an observable absence of tumor tissue in both flank tumors (Fig. 7) and mammary tumors (Fig. 8). The placebo formulation showed little or no observable effect in the tumor size or histology in either flank tumor when compared to control tumor tissue (Fig. 7) or mammary tumor (Fig. 8).

DISCUSSION

Since the discovery of paclitaxel two decades ago, significant work has been done to increase the bioavailability due to poor solubility through development of various delivery systems. We previously reported the use of a mucoadhesive nanoparticle formulation to increase the solubility of paclitaxel and subsequently increase the cellular accumulation and effectiveness of paclitaxel *in vitro* using MDA-MB-231 human breast cancer cells. The chitosan/GMO nanoparticulate formulation reported in previous studies incorporated paclitaxel in a chitosan/glyceryl monooleate (GMO) bioadhesive delivery system significantly increasing the cellular accumulation and efficacy of paclitaxel in MDA-MB-231 cells (20). The mean particle size of these nanoparticles were 432.5 ± 37.1 (mean ± SD; n = 3) with a mean zetapotential of (+)33.17 ± 1.52 (mean ± SD; n = 3). The

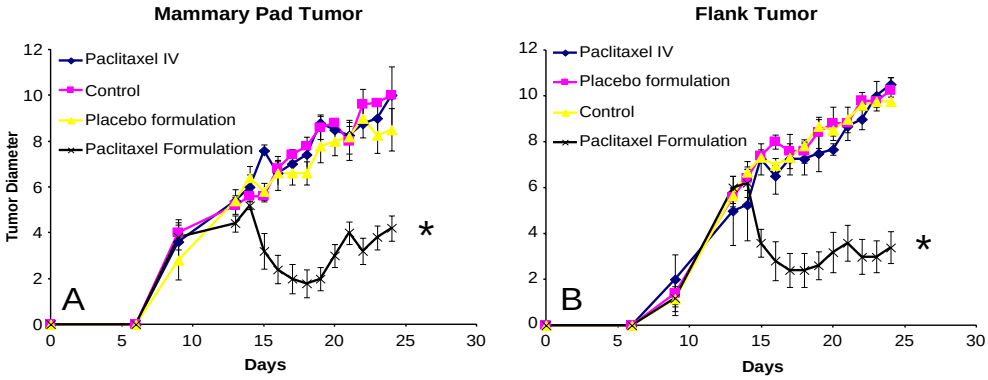

Fig. 5. Localized Chitosan/GMO formulation compared to a conventional formulation following systemic administration. The effectiveness of localized PTX formulated in a chitosan/GMO formulation was compared to systemic administration in SCID mice. **a**) Mammary pad tumors, **b**) flank tumors. Control mice (solid squares) received no treatment, PTX IV mice (solid diamonds) received PTX solution tail vein (15 mg/kg, for 3 days), Placebo group (solid triangles) received a single bolus local injection of a chitosan/GMO formulation without PTX (15 mg/kg formulation weight), and PTX formulation group (crosses) received a single bolus local injection of a chitosan/GMO formulation with PTX (15 mg/kg formulation weight). The tumor diameter data is expressed as mean ± SEM, n=6 animals. * considered significantly different $p<0.05$.

mean drug load determined using the HPLC method was 4.5% (w/w) ± 0.03 (mean ± SD; n = 3). These studies clearly demonstrated cell surface-bound of chitosan/GMO formulation. However, the evidence and mechanisms of internalization as well as the *in vivo* efficacy remained to be elucidated. The same mucoadhesive properties of chitosan have been shown effective in the delivery of various molecules in adenocarcinomas both *in vitro* and *in vivo* (15,16,22). Shikata and colleagues demonstrated increased cellular internalization of drug loaded chitosan nanoparticles in squamous cell carcinomas (SCC-VII) and melanoma cells (B16F10) when compared to drug solutions alone (22). The current report demonstrates both the *in vitro* cellular mechanism responsible for the increased cellular accumulation of the chitosan/GMO formulation and the *in vivo* efficacy of the chitosan/GMO formulation containing paclitaxel.

The cellular uptake and internalization of nanostructures have been extensively investigated for cell biology, imaging diagnostics and drug delivery. Confocal microscopic methods have been one of the modern methods in the determination of factors that effect sub-cellular localization of nanoparticles (23–31). Several physiochemical factors affecting cellular internalization of nanostructures have been identified including size and surface charge. Particles as large as 3 microns could be internalized by an order of magnitude larger than previously thought in phagocytic antigen-presenting cells (32,33). However, particles around 100 nm or smaller have been shown to have the most optimum rate of cellular uptake in epithelial cells and smooth muscle cells (34–36). The endocytosis pathway appears to be the predominate mechanism of cellular internalization of nanoparticles (30,35,36). The exposed surface charge significantly affected the ability of nanoparticles to internalize as well as the cellular endocytosis mechanism utilized. Negatively charged nanoparticles show an inferior rate of endocytosis and do not utilize the clathrin-mediated endocytosis pathway (37,38). On the other hand, positively charged nanoparticles

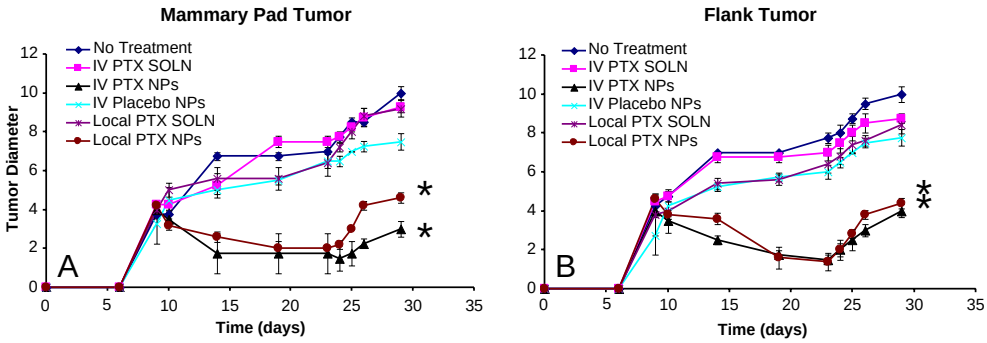

Fig. 6. Intravenous or localized chitosan/GMO formulation compared to a conventional formulation following systemic or localized administration. The effectiveness of localized PTX formulated in chitosan/GMO matrices was compared to systemic administration in SCID mice. **a**) Mammary pad tumors, **b**) flank tumors. Control mice received no treatment, PTX IV mice received PTX solution tail vein (15 mg/kg, for 3 days), PTX Local Solution (0.625 mg/kg), Placebo group received a tail vein injection of chitosan/GMO formulation without PTX (15 mg/kg formulation weight), and PTX formulation IV group received a tail vein injection of chitosan/GMO formulation with PTX (15 mg/kg formulation weight), and PTX Formulation local received a single bolus local injection of chitosan/GMO formulation with PTX (15 mg/kg formulation weight). The tumor diameter data is expressed as mean ± SEM, n=6 animals. * considered significantly different $p<0.05$.

Table I. The Anti-tumor Effects of PTX Chitosan/GMO Nanostructures

In Vivo Dosage Formulation	Rate of Tumor Growth (mm/day) Intravenous Study	Rate of Tumor Growth (mm/day) Localized Study
Control	0.344 ± 0.045	0.480 ± 0.039
Paclitaxel (PTX)	0.317 ± 0.034	0.457 ± 0.037
Placebo Chitosan/GMO	0.272 ± 0.035	0.457 ± 0.029
PTX Loaded Chitosan/GMO	0.054 ± 0.019	0.126 ± 0.038

The regression analysis of the tumor diameter presented as rate of tumor growth (mean ± SD, n=6)

internalize rapidly via the clathrin-mediated pathway (37,38). The current study, in agreement with these observations, clearly demonstrates significant rapid cellular accumulation of chitosan/GMO nanostructures through an endo-lysomal pathway. In addition, the findings in the current study also suggest that chitosan/GMO nanostructures escape from the lysosomes, and appear to partially co-localize in the nucleus and may result in a greater efficacy of a chemotherapeutic like paclitaxel. To date, nanoparticles similar or smaller than 100 nm have been shown to co-localize in the nuclear compartment (39–43). However, the particle size is much larger (~400 nm) in the current study. In separate studies, we previously evaluated this chitosan/GMO formulation in pancreatic cancer cells BXPC-3 and Mia PaCa-2 cells that showed similar rapid endo-lysomal internalization, but there was no nuclear co-localization observed (submitted manuscript). Together, the nuclear co-localization observed with chitosan/GMO nanostructures may be cell type dependent and further investigation is warranted. However, the internalization and sub-cellular localization of chitosan/GMO nanostructures in MDA-MB-231 cells may be one of the mechanisms attributed for the increased efficacy of paclitaxel observed in both the previous and the current studies.Several studies have shown increased *in vivo* efficacy with paclitaxel loaded nanoparticles when compared to commercial formulations of paclitaxel with Cremophor EL (44–57). Danheir and colleagues showed 3-fold lower IC50 of paclitaxel in human Cervix Carcinoma cells (HeLa) *in vitro* correlated to significant tumor growth inhibition compared to commercial formulations of paclitaxel (45). Hamaguchi and colleagues used a micellar nanoparticle formulation to enhance the anti-tumor activity and reduce the neuro-toxicity of paclitaxel. In these studies, the micellar formulation showed a 90-fold higher plasma AUC and

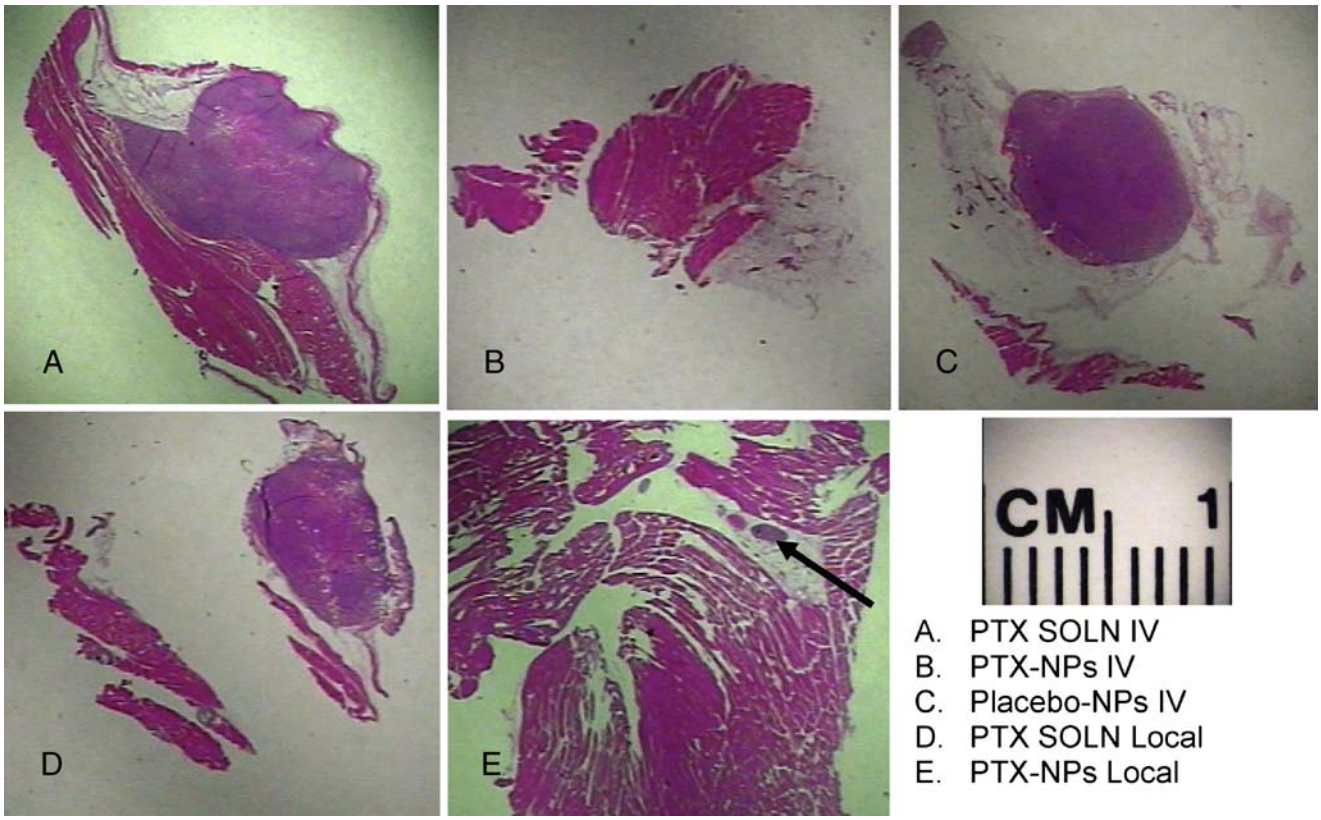

Fig. 7. End-point histological evaluation of intravenous or localized chitosan/GMO formulation compared to a conventional formulation following systemic or localized administration of flank xenograph MDA-MB-231 tumors in SCID mice at 28 days post-inoculation. **a**) PTX IV mice received PTX solution tail vein (15 mg/kg, qd for 3 days), **b**) PTX formulation IV group received a tail vein injection of chitosan/GMO formulation with PTX (15 mg/kg formulation weight), **c**) Placebo group received a tail vein injection of chitosan/GMO formulation without PTX (15 mg/kg formulation weight), **d**) PTX Local Solution (0.625 mg/kg), and E) PTX formulation local received a single bolus local injection of chitosan/GMO formulation with PTX (15 mg/kg formulation weight). The micrographs were collected under 10× magnification.

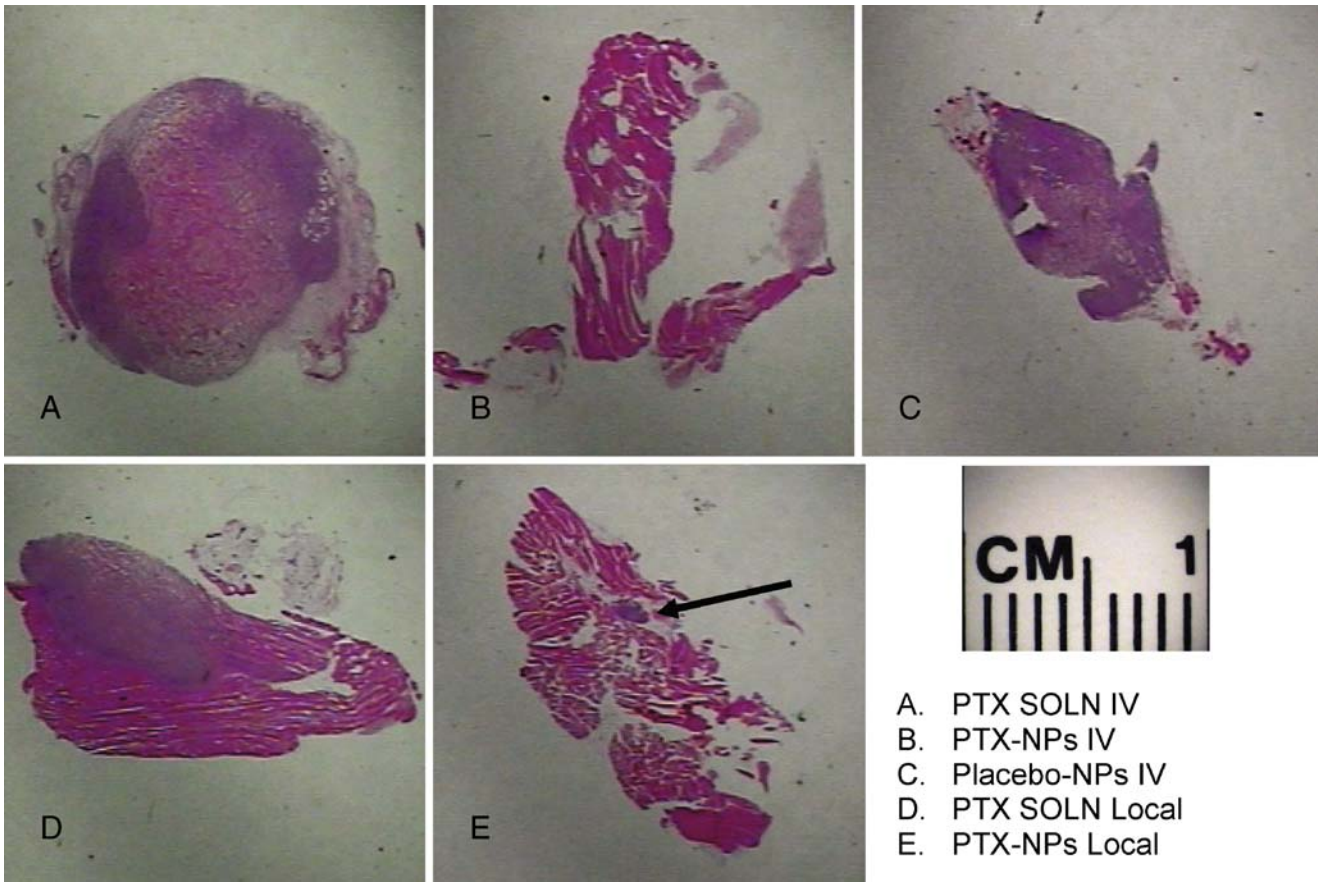

Fig. 8. End-point histological evaluation of intravenous or localized chitosan/GMO formulation compared to a conventional formulation following Systemic or localized administration of mammary xenograph MDA-MB-231 tumors in SCID mice at 28 days posth-inoculation. **a**) PTX IV mice received PTX solution tail vein (15 mg/kg, qd for 3 days), **b**) PTX formulation IV group received a tail vein injection of chitosan/GMO formulation with PTX (15 mg/kg formulation weight), **c**) Placebo group received a tail vein injection of chitosan/GMO formulation without PTX (15 mg/kg formulation weight), **d**) PTX Local Solution (0.625 mg/kg), and E) PTX Formulation local received a single bolus local injection of chitosan/GMO formulation with PTX (15 mg/kg formulation weight). The micrographs were collected under 10× magnification.

a 25-fold higher tumor AUC compared to free paclitaxel, that corresponded to significantly potent anti-tumor activity on a human colorectal cancer cell line HT-29 xenograph (57). Nornoo and Chow used phospholipids suspensions containing paclitaxel to eliminate Cremophor EL associated toxicities. In these studies, free paclitaxel (in Cremophor EL) had no effect on the growth of Colon-26 cells, a Taxol-resistant murine tumor, when given at doses that included or exceeded the maximum tolerated dose. However, the phospholipid liposome formulation significantly suppressed tumor progression (47). In addition, Yang and colleagues have shown significant antitumor activity in both BT-474 and MBA-MB-231 xenograft models with paclitaxel-loaded PEGylated immunoliposomes (PIL)(58). In these studies, they demonstrated increased antitumor activity with PIL compared to a solution of paclitaxel alone. These studies further show significant antitumor activity with the paclitaxel solution in PBS alone administered intravenously (58). However, this effect with the paclitaxel solution alone was not observed in the current studies. This observation may be related to differences in the dosage formulation of paclitaxel, in the cell culturing procedures and the mouse strain used. The current studies used a FOX-Chase SCID mouse and the conventional formulation of Taxol® in sterile water, where as Yang *et. al*. (2007) used Balb-c (nu/nu) mouse and taxol in PBS (58). In addition to this, Yang and colleagues cultured the MDA-MB-231 cells in DMEM media with high glucose compared to the current studies that used normal RPMI 1640 medium. It has been reported that hyperglycemic conditions promote increased paclitaxel cytotoxicity in MDA-MB-231 cells through thioredoxin activity *in vitro* (59). In support of this, studies by Han and colleagues (2005) reported only weak but detectable anticancer activity of paclitaxel in MDA-MB-231 cells cultured in RPMI 1640 inocculated in the mammary pad of Balb-c (nu/nu) mice following intraperitoneal injections (5 mg/kg weekly for 6 weeks)(60). The reasons for alterations in the efficacy of paclitaxel solutions alone remain unclear, and very difficult to speculate further. Despite these differences, the current studies also provide compelling *in vivo* evidence supporting the use of sustained delivery of paclitaxel with chitosan /GMO nanostructures to increase the efficacy of paclitaxel, and presumably, reduce the associated acute toxicities.

In the current studies, free paclitaxel (in Cremophor EL) showed little or no effect in the tumor progression of MDA-MB-231 xerograph tumors following either intra-tumor or studies intravenous administration in separate studies (Figs. 5 and 6). In contrast, the chitosan/GMO formulation with paclitaxel showed significant tumor growth progression at a significantly lower dose (20-times) when administered either intra-tumor or intravenous routes. In addition, chitosan/GMO formulation absent of paclitaxel had little effect on the tumor

progression. A regression analysis also confirms these observations (Table I). Furthermore, the tumor suppression of chitosan/GMO formulation containing paclitaxel is also confirmed through the end-point histopathological evaluation (Figs. 7 and 8). The fact that tumor suppression of the chitosan/GMO formulation containing paclitaxel following intra-tumor administration was similar to that of intravenous administration suggest that the delivery system is accumulating at the site of action. The histopathological results also may support the accumulation of the delivery system in the tumor following intravenous administration. In both flank and mammary xenograph sections, the absence of tumor tissue that was measured prior to histological processing probably suggest that the delivery system possibly melted during the paraffin polymerization process due to the low melting point of GMO (40ºC). Since these studies were end-point studies (10–20 days post-treatment), there was no measureable amounts of paclitaxel in the tumor tissues. However, the *in vivo* tumor tissue following treatment was isolated and cultured *in vitro*, and the cell micromorphology was similar to the original inoculation culture (unpublished observation). This observation confirms the absence of cystic tissue in the primary xenograph following treatment with chitosan/GMO containing paclitaxel. Together, these results provide support for the use of sustained delivery systems containing of paclitaxel to increase the efficacy of paclitaxel *in vivo*, and presumably, reduce associated acute toxicities.

CONCLUSIONS

Chitosan/GMO nanostructures can be formulated with paclitaxel to provide a delivery system that can easily re-suspend in aqueous media suitable for localized or intravenous administration. The localized or intravenous administration of lower doses of chitosan/GMO nanostructures containing paclitaxel significantly increases the anti-tumor activity of paclitaxel when compared to conventional paclitaxel formulations containing Cremophor EL. The increased anti-tumor activity associated with chitosan/GMO nanostructures is due to the time-dependent internalization and sub-cellular localization. The significant dose reduction of paclitaxel associated with chitosan/GMO nanostructures could be a method to reduce the acute toxicities in chemotherapy.

ACKNOWLEDGEMENTS

This work was partially supported by a Department of Defense Concept Award BC045664 and Health Future Foundations, Omaha, NE. This research was also partially conducted at the Integrative Biological Imaging Facility at Creighton University, Omaha, NE. This facility, supported by the C.U. Medical School, was constructed with support from C06 Grant RR17417-01 from the NCRR, NIH.

REFERENCES

1. Singla AK, Garg A, Aggarwal GD. Paclitaxel and its formulations. Int J Pharm. 2002;235:179–92. doi:10.1016/S0378-5173(01)00986-3.
2. Tarr BD, Yalkowsky SH. A new parenteral vehicle for the administration of some poorly soluble anti-cancer drugs. J Parenter Sci Technol. 1987;41:31–33.
3. Chao TC, Chu Z, Tseng LM, Chiou TJ, Hsieh RK, Wang WS, *et al*. Paclitaxel in a novel formulation containing less Cremophor EL as first-line therapy for advanced breast cancer: a phase II trial. Invest New Drugs. 2005;23:171–7. doi:10.1007/s10637-005-5863-8.
4. Gelderblom H, Verweij J, Nooter K, Sparreboom A. Cremophor EL: the drawbacks and advantages of vehicle selection for drug formulation. Eur J Cancer. 2001;37:1590–8. doi:10.1016/S0959-8049(01)00171-X.
5. Friedland D, Gorman G, Treat J. Hypersensitivity reactions from taxol and etoposide. J Natl Cancer Inst. 1993;85:2036. doi:10.1093/jnci/85.24.2036.
6. Rowinsky EK, Chaudhry V, Cornblath DR, Donehower RC. Neurotoxicity of Taxol. J Natl Cancer Inst Monogr. 1993;15:107–15.
7. Ibrahim NK, Desai N, Legha S, Soon-Shiong P, Theriault RL, Rivera E, *et al*. Phase I and pharmacokinetic study of ABI-007, a Cremophor-free, protein-stabilized, nanoparticle formulation of paclitaxel. Clin Cancer Res. 2002;8:1038–44.
8. Gradishar WJ. Albumin-bound paclitaxel: a next-generation taxane. Expert Opin Pharmacother. 2006;7:1041–53. doi:10.1517/14656566.7.8.1041.
9. Socinski M. Update on nanoparticle albumin-bound paclitaxel. Clin Adv Hematol Oncol. 2006;4:745–6.
10. Lee Villano J, Mehta D, Radhakrishnan L. Abraxane induced life-threatening toxicities with metastatic breast cancer and hepatic insufficiency. Invest New Drugs. 2006;24:455–6. doi:10.1007/s10637-006-6214-0.
11. Moore A, Medarova Z, Potthast A, Dai G. *In vivo* targeting of underglycosylated MUC-1 tumor antigen using a multimodal imaging probe. Cancer Res. 2004;64:1821–7. doi:10.1158/0008-5472.CAN-03-3230.
12. Sandri G, Bonferoni MC, Rossi S, Ferrari F, Gibin S, Zambito Y, *et al*. Nanoparticles based on N-trimethylchitosan: evaluation of absorption properties using *in vitro* (Caco-2 cells) and *ex vivo* (excised rat jejunum) models. Eur J Pharm Biopharm. 2007;65:68–77. doi:doi:10.1016/j.ejpb.2006.07.016.
13. Bernkop-Schnurch A, Weithaler A, Albrecht K, Greimel A. Thiomers: preparation and *in vitro* evaluation of a mucoadhesive nanoparticulate drug delivery system. Int J Pharm. 2006;317:76–81. doi:10.1016/j.ijpharm.2006.02.044.
14. Cui F, Qian F, Yin C. Preparation and characterization of mucoadhesive polymer-coated nanoparticles. Int J Pharm. 2006;316:154–61. doi:10.1016/j.ijpharm.2006.02.031.
15. Howard KA, Rahbek UL, Liu X, Damgaard CK, Glud SZ, Andersen MO, *et al*. RNA interference *in vitro* and *in vivo* using a novel chitosan/siRNA nanoparticle system. Mol Ther. 2006;14:476–84. doi:10.1016/j.ymthe.2006.04.010.
16. Zheng F, Shi XW, Yang GF, Gong LL, Yuan HY, Cui YJ, *et al*. Chitosan nanoparticle as gene therapy vector via gastrointestinal mucosa administration: results of an *in vitro* and *in vivo* study. Life Sci. 2007;80:388–96. doi:10.1016/j.lfs.2006.09.040.
17. Takeuchi H, Yamamoto H, Niwa T, Hino T, Kawashima Y. Enteral absorption of insulin in rats from mucoadhesive chitosan-coated liposomes. Pharm Res. 1996;13:896–901. doi:10.1023/A:1016009313548.
18. Takeuchi H, Thongborisute J, Matsui Y, Sugihara H, Yamamoto H, Kawashima Y. Novel mucoadhesion tests for polymers and polymer-coated particles to design optimal mucoadhesive drug delivery systems. Adv Drug Deliv Rev. 2005;57:1583–94. doi:10.1016/j.addr.2005.07.008.
19. Thongborisute J, Tsuruta A, Kawabata Y, Takeuchi H. The effect of particle structure of chitosan-coated liposomes and type of chitosan on oral delivery of calcitonin. J Drug Target. 2006;14:147–54. doi:10.1080/10611860600648346.
20. Trickler WJ, Nagvekar AA, Dash AK. A Novel Nanoparticle Formulation for Sustained Paclitaxel Delivery. AAPS PharmSciTech. 2008;9:486–93. doi:10.1208/s12249-008-9063-7.
21. Davda J, Labhasetwar V. Characterization of nanoparticle uptake by endothelial cells. Int J Pharm. 2002;233:51–9. doi:10.1016/S0378-5173(01)00923-1.
22. Shikata F, Tokumitsu H, Ichikawa H, Fukumori Y. *In vitro* cellular accumulation of gadolinium incorporated into chitosan nanoparticles designed for neutron-capture therapy of cancer. Eur J Pharm Biopharm. 2002;53:57–63. doi:10.1016/S0939-6411(01)00198-9.

23. Xu ZP, Niebert M, Porazik K, Walker TL, Cooper HM, Middelberg AP, *et al*. Subcellular compartment targeting of layered double hydroxide nanoparticles. J Control Release. 2008;130:86–94. doi:10.1016/j.jconrel.2008.05.021.
24. Yin M, Shen J, Gropeanu R, Pflugfelder GO, Weil T, Mullen K. Fluorescent core/shell nanoparticles for specific cell-nucleus staining. Small. 2008;4:894–8. doi:10.1002/smll.200701107.
25. Perumal OP, Inapagolla R, Kannan S, Kannan RM. The effect of surface functionality on cellular trafficking of dendrimers. Biomaterials. 2008;29:3469–76. doi:10.1016/j.biomaterials.2008.04.038.
26. Zou J, Saulnier P, Perrier T, Zhang Y, Manninen T, Toppila E, et al. Distribution of lipid nanocapsules in different cochlear cell populations after round window membrane permeation. J Biomed Mater Res B Appl Biomater. 2008;87:10–8.
27. de la Fuente M, Seijoand B, Alonso MJ. Bioadhesive hyaluronan-chitosan nanoparticles can transport genes across the ocular mucosa and transfect ocular tissue. Gene Ther. 2008;15:668–76. doi:10.1038/gt.2008.16.
28. Lacoeuille F, Garcion E, Benoit JP, Lamprecht A. Lipid nanocapsules for intracellular drug delivery of anticancer drugs. J Nanosci Nanotechnol. 2007;7:4612–7.
29. Zhang LW, Yu WW, Colvin VL, Monteiro-Riviere NA. Biological interactions of quantum dot nanoparticles in skin and in human epidermal keratinocytes. Toxicol Appl Pharmacol. 2008;228:200–11. doi:10.1016/j.taap. 2007.12.022.
30. Panyam J, Labhasetwar V. Targeting intracellular targets. Curr Drug Deliv. 2004;1:235–47. doi:10.2174/1567201043334768.
31. Panyam J, Zhou WZ, Prabha S, Sahoo SK, Labhasetwar V. Rapid endo-lysosomal escape of poly(DL-lactide-co-glycolide) nanoparticles: implications for drug and gene delivery. Faseb J. 2002;16:1217–26. doi:10.1096/fj.02-0088com.
32. Erni C, Suard C, Freitas S, Dreher D, Merkle HP, Walter E. Evaluation of cationic solid lipid microparticles as synthetic carriers for the targeted delivery of macromolecules to phagocytic antigen-presenting cells. Biomaterials. 2002;23:4667–76. doi:10.1016/S0142-9612(02)00216-8.
33. Koval M, Preiter K, Adles C, Stahl PD, Steinberg TH. Size of IgG-opsonized particles determines macrophage response during internalization. Exp Cell Res. 1998;242:265–73. doi:10.1006/excr.1998.4110.
34. Costanzo PJ, Patten TE, Seery TA. Nanoparticle agglutination: acceleration of aggregation rates and broadening of the analyte concentration range using mixtures of various-sized nanoparticles. Langmuir. 2006;22:2788–94. doi:10.1021/la0522909.
35. Chavanpatil MD, Khdair A, Panyam J. Nanoparticles for cellular drug delivery: mechanisms and factors influencing delivery. J Nanosci Nanotechnol. 2006;6:2651–63. doi:10.1166/jnn.2006.443.
36. Panyam J, Labhasetwar V. Dynamics of endocytosis and exocytosis of poly(D, L-lactide-co-glycolide) nanoparticles in vascular smooth muscle cells. Pharm Res. 2003;20:212–20. doi:10.1023/A:1022219003551.
37. Harush-Frenkel O, Rozentur E, Benita S, Altschuler Y. Surface charge of nanoparticles determines their endocytic and transcytotic pathway in polarized MDCK cells. Biomacromolecules. 2008;9:435–43. doi:10.1021/bm700535p.
38. Harush-Frenkel O, Debotton N, Benita S, Altschuler Y. Targeting of nanoparticles to the clathrin-mediated endocytic pathway. Biochem Biophys Res Commun. 2007;353:26–32. doi:10.1016/j.bbrc.2006.11.135.
39. Xu P, Van Kirk EA, Zhan Y, Murdoch WJ, Radosz M, Shen Y. Targeted charge-reversal nanoparticles for nuclear drug delivery. Angew Chem Int Ed Engl. 2007;46:4999–5002. doi:10.1002/anie.200605254.
40. Berry CC, de la Fuente JM, Mullin M, Chu SW, Curtis AS. Nuclear localization of HIV-1 tat functionalized gold nanoparticles. IEEE Trans Nanobioscience. 2007;6:262–9. doi:10.1109/TNB.2007.908973.
41. Ryan JA, Overton KW, Speight ME, Oldenburg CN, Loo L, Robarge W, *et al*. Cellular uptake of gold nanoparticles passivated with BSA-SV40 large T antigen conjugates. Anal Chem. 2007;79:9150–9. doi:10.1021/ac0715524.
42. Tkachenko AG, Xie H, Liu Y, Coleman D, Ryan J, Glomm WR, *et al*. Cellular trajectories of peptide-modified gold particle complexes: comparison of nuclear localization signals and peptide transduction domains. Bioconjug Chem. 2004;15:482–90. doi:10.1021/bc034189q.
43. Tkachenko AG, Xie H, Coleman D, Glomm W, Ryan J, Anderson MF, *et al*. Multifunctional gold nanoparticle-peptide complexes for nuclear targeting. J Am Chem Soc. 2003;125:4700–1. doi:10.1021/ja0296935.
44. Mugabe C, Hadaschik BA, Kainthan RK, Brooks DE, So AI, Gleave ME, Burt HM. Paclitaxel incorporated in hydrophobically derivatized hyperbranched polyglycerols for intravesical bladder cancer therapy. *BJU Int* (2008)
45. Danhier F, Lecouturier N, Vroman B, Jerome C, Marchand-Brynaert J, Feron O, *et al*. Paclitaxel-loaded PEGylated PLGA-based nanoparticles: *in vitro* and *in vivo* evaluation. J Control Release. 2009;133:11–7. doi:10.1016/j.jconrel.2008.09.086.
46. Zhang Z, Lee SH, Gan CW, Feng SS. *In vitro* and *in vivo* investigation on PLA-TPGS nanoparticles for controlled and sustained small molecule chemotherapy. Pharm Res. 2008;25:1925–35. doi:10.1007/s11095-008-9611-6.
47. Nornoo AO, Chow DS. Cremophor-free intravenous microemulsions for paclitaxel II. Stability, *in vitro* release and pharmacokinetics. Int J Pharm. 2008;349:117–23. doi:10.1016/j.ijpharm.2007.07.043.
48. Dong Y, Feng SS. *In vitro* and *in vivo* evaluation of methoxy polyethylene glycol-polylactide (MPEG-PLA) nanoparticles for small-molecule drug chemotherapy. Biomaterials. 2007;28:4154–60. doi:10.1016/j.biomaterials.2007.05.026.
49. Lee SW, Chang DH, Shim MS, Kim BO, Kim SO, Seo MH. Ionically fixed polymeric nanoparticles as a novel drug carrier. Pharm Res. 2007;24:1508–16. doi:10.1007/s11095-007-9269-5.
50. Koziara JM, Whisman TR, Tseng MT, Mumper RJ. *In-vivo* efficacy of novel paclitaxel nanoparticles in paclitaxel-resistant human colorectal tumors. J Control Release. 2006;112:312–9. doi:10.1016/j.jconrel.2006.03.001.
51. Win KY, Feng SS. *In vitro* and *in vivo* studies on vitamin E TPGS-emulsified poly(D, L-lactic-co-glycolic acid) nanoparticles for paclitaxel formulation. Biomaterials. 2006;27:2285–91. doi:10.1016/j.biomaterials.2005.11.008.
52. Chen DB, Yang TZ, Lu WL, Zhang Q. *In vitro* and *in vivo* study of two types of long-circulating solid lipid nanoparticles containing paclitaxel. Chem Pharm Bull (Tokyo). 2001;49:1444–7. doi:10.1248/cpb.49.1444.
53. Sharma D, Chelvi TP, Kaur J, Chakravorty K, De TK, Maitra A, *et al*. Novel Taxol formulation: polyvinylpyrrolidone nanoparticle-encapsulated Taxol for drug delivery in cancer therapy. Oncol Res. 1996;8:281–6.
54. Wang Y, Li Y, Zhang L, Fang X. Pharmacokinetics and biodistribution of paclitaxel-loaded pluronic P105 polymeric micelles. Arch Pharm Res. 2008;31:530–8. doi:10.1007/s12272-001-1189-2.
55. Han LM, Guo J, Zhang LJ, Wang QS, Fang XL. Pharmacokinetics and biodistribution of polymeric micelles of paclitaxel with Pluronic P123. Acta Pharmacol Sin. 2006;27:747–53. doi:10.1111/j.1745-7254.2006.00340.x.
56. Kim SC, Kim DW, Shim YH, Bang JS, Oh HS, Wan Kim S, *et al*. *In vivo* evaluation of polymeric micellar paclitaxel formulation: toxicity and efficacy. J Control Release. 2001;72:191–202. doi:10.1016/S0168-3659(01)00275-9.
57. Hamaguchi T, Matsumura Y, Suzuki M, Shimizu K, Goda R, Nakamura I, *et al*. NK105, a paclitaxel-incorporating micellar nanoparticle formulation, can extend *in vivo* antitumour activity and reduce the neurotoxicity of paclitaxel. Br J Cancer. 2005;92:1240–6. doi:10.1038/sj.bjc.6602479.
58. Yang T, Choi MK, Cui FD, Lee SJ, Chung SJ, Shim CK, *et al*. Antitumor effect of paclitaxel-loaded PEGylated immunoliposomes against human breast cancer cells. Pharm Res. 2007;24:2402–11. doi:10.1007/s11095-007-9425-y.
59. Turturro F, Von Burton G, Friday E. Hyperglycemia-induced thioredoxin-interacting protein expression differs in breast cancer-derived cells and regulates paclitaxel IC50. Clin Cancer Res. 2007;13:3724–30. doi:10.1158/1078-0432.CCR-07-0244.
60. Han GZ, Liu ZJ, Shimoi K, Zhu BT. Synergism between the anticancer actions of 2-methoxyestradiol and microtubule-disrupting agents in human breast cancer. Cancer Res. 2005;65:387–93.